Biochimica et Biophysica Acta 1818 (2012) 1291–1301

Contents lists available at SciVerse ScienceDirect

Biochimica et Biophysica Acta

journal homepage: www.elsevier.com/locate/bbamem

Ceramide channels: Influence of molecular structure on channel formation in membranes

Meenu N. Perera [a,1], Vidyaramanan Ganesan [a,1], Leah J. Siskind [b,c], Zdzislaw M. Szulc [c], Jacek Bielawski [c], Alicja Bielawska [c], Robert Bittman [d], Marco Colombini [a,*]

[a] University of Maryland, College Park, MD 20742, USA
[b] Ralph H. Johnson Veterans Affairs Medical Center, Charleston, SC 29401, USA
[c] Medical University of South Carolina, Charleston, SC 29403, USA
[d] City University of New York, Queens College, NY 11367, USA

ARTICLE INFO

Article history:
Received 21 November 2011
Received in revised form 8 February 2012
Accepted 9 February 2012
Available online 15 February 2012

Keywords:
Ceramide
Analogs
Channels
Mitochondria
Permeabilization
Pore

ABSTRACT

The sphingolipid, ceramide, self-assembles in the mitochondrial outer membrane (MOM), forming large channels capable of translocating proteins. These channels are believed to be involved in protein release from mitochondria, a key decision-making step in cell death. Synthetic analogs of ceramide, bearing modifications in each of the major structural features of ceramide were used to probe the molecular basis for the stability of ceramide channels. Channel stability and mitochondrial permeabilization were disrupted by methylation of the C1-hydroxyl group whereas modifications of the C3 allylic hydroxyl group were well tolerated. A change in chirality at C2 that would influence the orientation of the C1-hydroxyl group resulted in a strong reduction of channel-forming ability. Similarly, methylation of the amide nitrogen is also detrimental to channel formation. Many changes in the degree, location and nature of the unsaturation of ceramide had little effect on mitochondrial permeabilization. Competition experiments between ceramide and analogs resulted in synergy with structures compatible with the ceramide channel model and antagonism with incompatible structures. The results are consistent with ceramide channels being highly organized structures, stabilized by specific inter-molecular interactions, similar to the interactions responsible for protein folding.

1. Introduction

The sphingolipid, ceramide, has been shown to be able to form channels in planar membranes [1], liposomes [2] and the mitochondrial outer membrane [3,4]. In mammalian mitochondria, channel formation occurs at physiologically relevant ceramide levels [4]; levels measured in mitochondria from cells early in the apoptotic process [5–7]. In addition, the propensity to form channels and their size is influenced by Bcl-2 family proteins [8,9]. These channels are large, stable and capable of allowing proteins to cross membranes [3,4]. The size was determined from the molecular weight of proteins released from mitochondria [3], from the conductance of single channels formed in planar membranes [10], and from visualization of the pores by electron microscopy [11]. A range of sizes was reported with a typical channel having an estimated pore diameter of 10 nm [10,11]. Thus hundreds of ceramide molecules must spontaneously self-assemble in the 2-dimensional liquid phase of the membrane. Unlike the fluid and transient toroidal pores or lipidic pores formed when lamellar lipids are disturbed by amphipathic molecules such as peptides or synthetic structures [12–14], whole proteins [15,16], or at the phase transition [17], the channels formed by ceramide seem to be highly structured and rigid. The disassembly of channels formed by short-chain ceramide shows a quantization of conductance with a strong preference for large conductance drops to be multiples of 4 nS [10]. This finding not only supports the notion that ceramide channels are highly-organized cylindrical structures, but is also consistent with a modification of the originally-proposed barrel-stave structure [1]. Each stave of the barrel is proposed to consist of a stack of ceramide molecules held together by intermolecular hydrogen-bonding through the amide and carbonyl groups of the amide linkage. These span the membrane forming a cylinder when arranged in an anti-parallel fashion (supplemental Fig. 1S) [10]. Molecular dynamic simulations indicate that this structure is stable [18].

The ability of ceramide to form channels must, at least in part, be attributed to the structural features of the ceramide molecule. The polar head group of ceramide (Fig. 1), with its amide linkage and two hydroxyl groups located in close proximity, constitutes a tridentate hydrogen-bonding donor/acceptor center and is capable of

Abbreviations: D-e-, D-*erythro*-; L-e-, L-*erythro*-; C_8-Cer, D-e-C_8-ceramide; C_{16}-Cer, D-e-C_{16}-ceramide; $C_{18:1}$-Cer, D-e-$C_{18:1}$-ceramide; DNP, 2,4-dinitrophenol; BSA, fatty acid depleted bovine serum albumin; MOM, mitochondrial outer membrane; DPX, p-xylene-bis-pyridinium bromide

* Corresponding author at: Department of Biology, University of Maryland, College Park, MD, 20742, USA. Tel.: +1 301 405 6925; fax: +1 301 314 9358.
E-mail address: colombini@umd.edu (M. Colombini).

[1] These authors contributed equally to the work.

0005-2736/$ – see front matter © 2012 Elsevier B.V. All rights reserved.
doi:10.1016/j.bbamem.2012.02.010

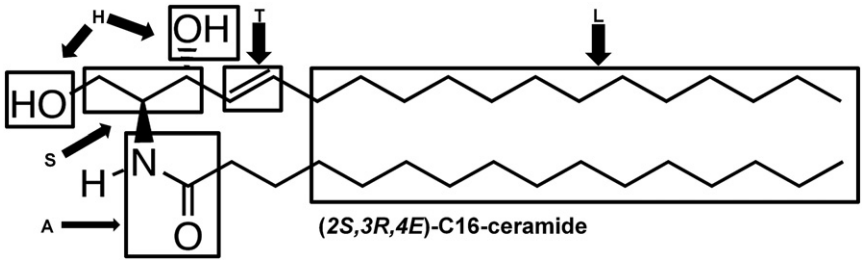

Fig. 1. Structure of *N*-palmitoyl-D-*erythro*-sphingosine (D-e-C_{16}-ceramide or C_{16}-Cer) showing the major features of the molecule and the codes used for the synthetic analogs: **H** for changes to the hydroxyl groups, **S** for changes in stereochemistry, **A** for changes to the amide group, **T** for changes to the *trans* double bond and **L** for changes to the chain length.

generating an effective network of directed hydrogen bonding interactions. These structural features may partly explain its ability to form large, stable channels in membranes. However, it is not known if the location and orientation of the interacting groups are critical to achieve a stable structure. In addition, other structural features (such as the length of the hydrocarbon chains and the number and configuration of the double bonds) may be important. Therefore, we have undertaken a study of synthetic ceramide analogs (Table 1, Fig. 2) to determine (a) if naturally occurring ceramides are uniquely suited to form large aqueous pores and (b) the structural and stereochemical features in ceramide that are necessary for the formation of large channels.

2. Materials and methods

2.1. Reagents

N-Palmitoyl-D-*erythro*-sphingosine (D-e-C_{16}-ceramide or C_{16}-Cer) and *N*-oleoyl-D-*erythro*-sphingosine (D-e-$C_{18:1}$-ceramide or $C_{18:1}$-Cer) were obtained from Avanti Polar Lipids (Alabaster, AL). The analogs of C_{16}-Cer and D-e-C_8-ceramide (C_8-Cer) and **{T1, T4}** (Fig. 2) were synthesized as described previously [19–26]. Antimycin A, 2,4-dinitrophenol (DNP), horse heart cytochrome c, and fatty acid depleted bovine serum albumin (BSA) were purchased from Sigma (St. Louis, MO). DPX (p-xylene-bis-pyridinium bromide) was purchased from Molecular Probes (Invitrogen). 5(6)-carboxyfluorescein was purchased from Acros Organics.

2.2. Preparation of rat liver mitochondria

Rat liver mitochondria were isolated by differential centrifugation of tissue homogenates as described previously [27] as modified [3]. Briefly, male Sprague–Dawley rats were fasted overnight and sacrificed by decapitation. The liver was excised and minced in cold isolation medium, H buffer (70 mM sucrose, 210 mM mannitol, 0.1 mM EGTA, 5.0 mM HEPES, pH 7.5), supplemented with 0.5% (w/v) fatty-acid depleted BSA followed by homogenization in a motorized Potter–Thomas Teflon-glass homogenizer (two passes). The homogenate was subjected to 10-min cycles of low speed (600*g*) and high speed (8600*g*) centrifugations in the same medium (twice each) at 4 °C in a Sorvall SS-34 rotor. After the low speed spin, the supernatant was collected and spun at high speed. The pellet obtained after the high speed centrifugation was resuspended in the medium of the same composition and centrifuged. BSA was removed by centrifugation at 8600*g* in BSA-free medium. The final mitochondrial pellet was resuspended in an ice cold sucrose free isotonic buffer FH (280 mM mannitol, 0.1 mM EGTA, 2 mM HEPES, pH 7.4). The mitochondrial intactness was determined from the rate of cytochrome *c* oxidation (vide infra) compared with the rate measured after mild hypotonic shock [28].

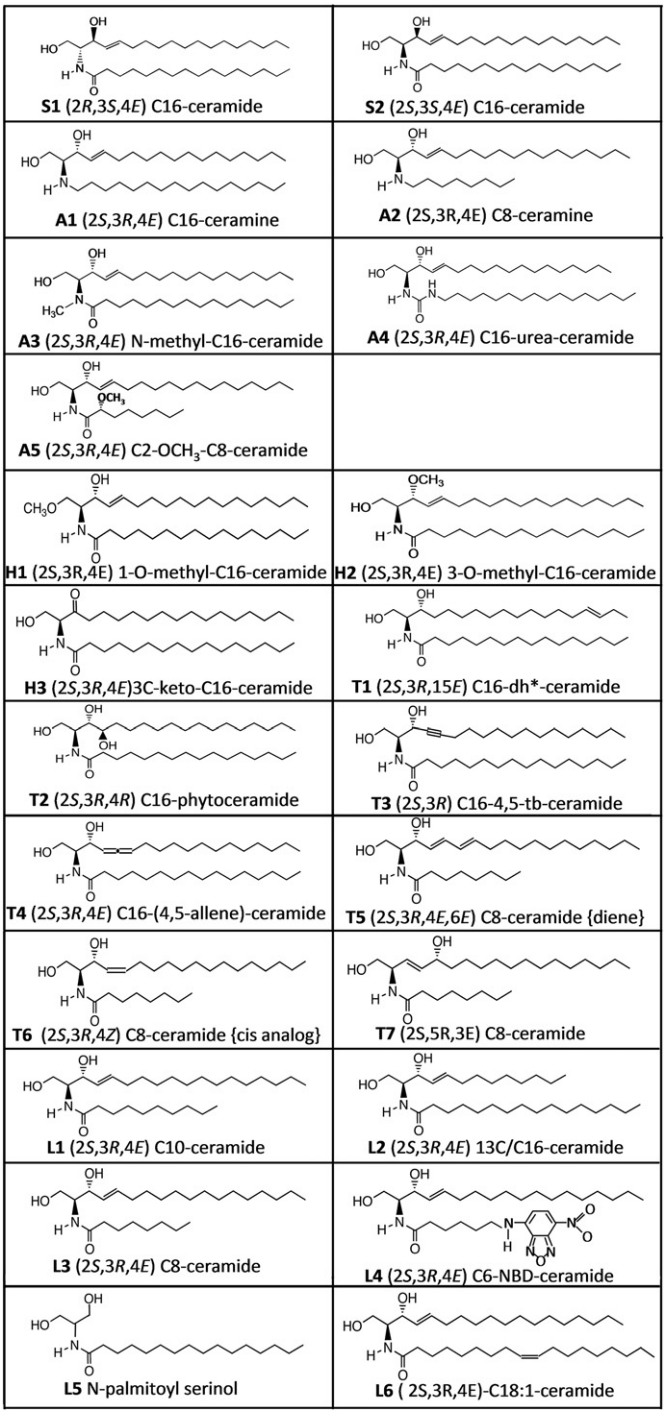

Fig. 2. Chemical structures of the analogs used.

2.3. Preparation of cytochrome c

Horse heart cytochrome *c* (2 mM) was reduced by an excess of reducing agent, ascorbate (40 mM), 0.2 M Tris-Cl (pH 7.5). The reduced cytochrome *c* was separated from ascorbate by using Sephadex G-10 gel filtration [3]. The concentration of reduced cytochrome *c* was determined spectrophotometrically from the absorbance at 550 nm.

2.4. Cytochrome c oxidation assay as a measure of mitochondrial outer membrane permeability

The rate of oxidation of exogenously-added reduced cytochrome *c* by cytochrome oxidase in isolated mitochondria is a measure of the permeability of the outer membrane to cytochrome *c* because translocation of cytochrome *c* through the outer membrane is a rate limiting step (see Fig. 2S). The procedure previously described [29] was modified to improve reproducibility. As the mitochondria were found to be more stable at higher concentrations, mitochondria were diluted in H buffer at 4 °C to a concentration of 0.2 mg/mL, in small batches just before the assay. Then, 50 μL aliquots were dispersed in 650 μL of room temperature H buffer supplemented with 5 mM DNP and 5 μM antimycin A. The final protein concentration was 14.3 μg/mL. The mitochondria were allowed to acclimate at room temperature (10 min) in a microfuge tube. Then ceramide or one of the analogs (dissolved in 2-propanol at 1 mg/mL) was delivered to the mitochondria while the suspension was vortexed for 30 s to achieve effective dispersal of the sphingolipid. After dispersal, the mixture was incubated for 10 min at room temperature followed by addition of cytochrome *c* (20 μL; final concentration, approx. 25 μM) and immediate measurement of the absorbance at 550 nm for a period of 2 min. The initial rate of decline of absorbance of reduced cytochrome *c* was used as a measure the permeability of the outer membrane to cytochrome *c*; ε_{550} (red-ox) = 18.5 $mM^{-1}\,cm^{-1}$. Vehicle controls were treated in an identical way. The percent of mitochondria with intact MOMs in these experiments was greater than 85%. Rates were corrected for the rate of oxidation observed with vehicle alone and this was very close to the untreated rate arising from a small number of damaged mitochondria.

The sensitivity of isolated mitochondria to permeabilization by added ceramide or analogs varied from one preparation to another. Therefore experiments with analogs were always performed in parallel with experiments with C_{16}-Cer. In this way the permeabilization produced by the analog (measures as the rate of cytochrome c oxidation) could be compared to that of C_{16}-Cer, either directly by reporting both rates or by expressing the result as a percent of that observed with C_{16}-Cer (Table 2).

The degree of cooperativity between an analog and C_{16}-Cer was determined by averaging the rate of cytochrome c oxidation achieved with a specific amount of each agent alone (called the "expected average") and comparing this with the rate observed with half the amount of each agent added combined (called the "combined effect"). The degree of cooperativity is expressed as the ratio of the combined effect to the expected average. A result not significantly different from "1" means no cooperativity; greater than "1" is synergy; less than "1" is antagonism.

Table 1
Ceramide analogs.

Code	Structural change	Type/location of change
S1	enantiomer: 2*S*,3*R* to 2*R*,3*S*	Stereochemical
S2	diastereomer: 3*R* to 3*S*	
A1	C_{16}-ceramine (conversion of amide chain to amine-linked chain)	amide linkage
A2	C_8-ceramine	
A3	*N*-methylation of amide chain	
A4	urea-ceramide	
A5	α-methoxy group in amide chain of C_8-ceramide	
H1	*O*-methylation of C1-hydroxyl group	hydroxyl group
H2	*O*-methylation of C3-hydroxyl group	
H3	oxidation of C3-OH to keto group; no double bond	
T1	translocation of double bond on sphingoid base	*trans* double bond
T2	phytoceramide: double bond replaced by OH at C4	
T3	double bond converted to triple bond	
T4	allene: adjacent double bonds	
T5	4,6-diene: conjugated *trans* double bonds in C_8-ceramide	
T6	*trans* double bond converted to *cis* in C_8-ceramide	
T7	translocation of double bond and C3-OH in C_8-ceramide	
L1	C_{10}-ceramide	hydrocarbon chains
L2	truncation of sphingoid base	
L3	C_8-ceramide	
L4	NBD-ceramide	
L5	*N*-palmitoyl-serinol	
L6	*N*-oleoyl-ceramide ($C_{18:1}$)	

2.5. Measurement of adenylate kinase release

The assay was performed as described earlier [30]. Mitochondrial suspensions containing 160 μg of mitochondrial protein were resuspended in isotonic buffer to a final volume of 1 mL. After the mitochondria were acclimated at room temperature for 10 min, ceramide or the analog was added, while vortexing. The mitochondria were incubated for 10 min at room temperature followed by centrifugation (14,000*g*) for 5 min at 4 °C (Beckman Coulter Microfuge 22R Centrifuge). A portion of the supernatant (300 μL) was combined with adenylate kinase reaction mixture (700 μL; 50 mM Tris, 5 mM $MgSO_4$, 10 mM glucose, 5 mM ADP, 0.2 mM NADP, pH 7.5) that had been preincubated for 2 min with enzyme mixture (5 μL; 2.5 units of hexokinase and 8.7 units of glucose 6-phosphate dehydrogenase) to consume ATP present in the reaction mixture prior to addition of the supernatant. The absorbance increase at 340 nm, from the generation of NADPH, was measured over 2 min. The maximal release was determined by measuring the activity of the supernatant obtained from an equal amount of osmotically shocked mitochondria. Measurement of adenylate kinase release does not measure the mitochondrial outer membrane (MOM) permeability but rather detects that, at some point after treatment, the MOM was made permeable (perhaps transiently) to this 26 kDa protein.

2.6. Measurement of lipid insertion into mitochondria

C_{16}-Cer, one of the analogs, or a combination of both was added to a 0.7 mL mitochondrial suspension containing 160 μg of mitochondrial protein in H buffer. In each experiment 30 μL of a 1 mg/mL 2-propanol solution of the lipid(s) was added while vortexing as described above. The suspension was then layered on 0.7 mL of ice-cold solution of 15% (w/v) sucrose, 5 mM HEPES pH 7.5 and centrifuged at 18,000*g* for 5 min at 4 °C. (Beckman Coulter Microfuge 22R Centrifuge). The mitochondria pelleted and the uninserted lipid remained out of the sucrose layer. (Prior experiments showed that dispersed ceramide floats at this density [11]) Most of the supernatant was aspirated gradually and the tube inverted and any liquid wiped off with paper wiper. The pellets were used for lipid extraction and measurement of the mitochondria incorporated ceramide and analogs by LC-MS/MS as previously described [31,32].

2.7. Liposome permeabilization

Single-walled liposomes (93% asolectin and 7% cholesterol, by weight) were prepared by the extrusion method as previously

Table 2
Relative potency of analogs to permeabilize the mitochondrial outer membrane. MOM was permeabilized by the addition of the indicated amount of analog (nmoles of analog per μg of mitochondrial protein) and the degree of permeabilization, as measured by the rate of cytochrome c oxidation is expressed as a percent (± S.E. of at least 3 trials) of the permeabilization measured in parallel experiments with C_{16}-Cer. The *P* values indicate the statistical significance of the permeabilization compared to that observed with C_{16}-Cer using the Student's *t* test. N/D means not done. N/S means not significantly different at the 95% confidence level.

Compound	Code	% of C_{16}-Cer permeabilization at 0.5–1 nmol/μg protein	*P* value	% of C_{16}-Cer permeabilization at 3 nmol/μg protein	*P* value	% of C_{16}-Cer partitioning from Table 3
(2*R*,3*S*,4*E*) C_{16}-ceramide	S1	No effect ($P=0.32$ relative to vehicle control)	<0.01	16 ± 4	<0.01	40
(2*S*,3*S*,4*E*) C_{16}-ceramide	S2	40 ± 60	N/S	80 ± 9	<0.05	–
(2*S*,3*R*,4*E*) *N*-methyl-C_{16}-ceramide	A3	No effect ($P=0.41$ relative to vehicle control)	<0.02	21 ± 4	<0.01	75
(2*S*,3*R*,4*E*) C16-urea-ceramide	A4	236 ± 35	N/S	229 ± 7	<0.005	–
(2*S*,3*R*,4*E*) 3-*O*-methyl-C_{16}-ceramide	H2	125 ± 3	N/S	107 ± 15	N/S	60
(2*S*)-3-keto-C_{16}-dh-ceramide	H3	N/D		320 ± 82	<0.01	–
(2S,3R,15*E*) C_{16}-dh-ceramide	T1	76 ± 4	<0.03	385 ± 59	<0.001	30
(2*S*,3*R*,4*R*) C_{16}-phytoceramide	T2	429 ± 27	<0.03	230 ± 50	<0.05	460
(2*S*,3*R*) C_{16}-4,5-tb-ceramide	T3	N/D		120 ± 20	N/S	–
(2*S*,3*R*,4*E*) C_{16}-(4,5-allene)-ceramide	T4	N/D		303 ± 26	<0.02	–
(2*S*,3*R*,4*E*) C_{10}-ceramide	L1	46 ± 17	<0.02	662 ± 26	<0.005	90
(2*S*,3*R*,4*E*) 13C/C_{16}-ceramide	L2	1310 ± 104	<0.005	606 ± 27	<0.005	–
N-palmitoyl-serinol	L5	N/D		306 ± 92	<0.01	–
(2*S*,3*R*,4*E*)$C_{18:1}$-ceramide	L6	100 ± 19	N/S	113 ± 4	N/S	–

described [2]. In summary, lipids (total mass, 5 mg) were hydrated in a buffer containing 1.5 mM carboxyfluorescein (CF), 6 mM DPX, 38.8 mM NaCl, 10 mM HEPES, and 1 mM EDTA, pH 7.0. The mixture was vortexed and subjected to 4 cycles of freeze–thaw-sonication followed by freeze–thawing and extrusion through a polycarbonate membrane (13 times) to form uniform single walled vesicles (100 nm diameter). A Sephacryl S200 gel filtration column (1.5 cm × 30 cm) was used to separate the liposomes from untrapped fluorophore using an isoosmotic elution buffer lacking carboxyfluorescein and DPX (50 mM NaCl, 10 mM HEPES, 1 mM EDTA, pH 7.0). Aliquots (100 μL; containing approximately 0.1 mg of lipid) of the liposome suspension were diluted into 2 mL of the eluting buffer. CF was excited at 495 nm and the emitted light was detected at 520 nm in a Deltascan spectrofluorometer (Photon Technology Instruments). The fluorescence intensity was measured as a function of time under constant stirring and the test compound was added. The increase in fluorescence intensity was the result of the release of CF from the liposomes and its dilution from the quenching agent, DPX. The maximal increase in fluorescence intensity was measured after the addition of 150 μL of 5% Triton-X 100. The liposome permeabilization was plotted as % release of CF relative to maximal release.

2.8. Channel formation in planar membranes

Electrophysiological studies were conducted on some of the analogs to determine whether they were able to permeabilize planar phospholipid membranes devoid of proteins or other mitochondrial factors. Planar phospholipid membranes were generated using the monolayer method as previously described [33] and modified [34]. The lipids comprising the monolayers were 1,2-diphytanoyl-sn-glycero-3-phosphocholine, asolectin, and cholesterol at a 1:1:0.1 ratio by weight. The aqueous solutions were 1.0 M KCl, 1 mM $MgCl_2$, 5 mM PIPES pH 6.9 on both sides of the chamber. The bilayer was formed across a 100 μm diameter hole in a Saran partition. Calomel electrodes were used to interface with the aqueous solution, the voltage was clamped and the current recorded. To form a channel, successive additions of 5–20 μL of 0.05 mg/mL of the analog in 2-propyl alcohol were stirred into the aqueous solution (5 mL) on one side of the membrane. The vehicle has no effect and its final concentration was less that 1% (v/v).

3. Results

The analogs were tested for their ability to permeabilize the outer membrane of isolated rat liver mitochondria to proteins, using the cytochrome *c* oxidation assay (Fig. 2S). Permeation through the MOM limits the rate of oxidation of exogenously-added cytochrome *c* by cytochrome oxidase in the inner membrane and thus the initial rate of oxidation cytochrome *c* was utilized as a measure of the permeabilization of the MOM to proteins. Sample dose–response curves are shown in Fig. 3. Note that the shapes of these curves vary from rectangular hyperbola to sigmoid, making rigorous comparisons difficult. Generally a dose of 30 nmol per 10 μg of mitochondrial protein was chosen as the common dose for comparison because it was low enough to avoid pronounced saturation by some analogs but high enough to detect permeabilization by the less-effective analogs. Results with lower doses are also reported. The sensitivity of mitochondria to MOM permeabilization varied from one isolation to the next so the permeabilization results summarized in Table 2 are expressed as a percentage of the permeabilization achieved by ceramide in the same mitochondrial preparation, either C_{16}-Cer or C_8-Cer, as appropriate.

An indication of MOM permeabilization was also obtained by measuring the extent of release of adenylate kinase. This is not a measure of MOM permeabilization but rather an indication of the fraction of mitochondria that have been permeabilized. With one notable outlier (vide infra) the MOM permeabilization assay and the adenylate kinase release assay yielded similar results for the analogs when compared to the effect of ceramide (Fig. 4). The permeabilizing ability of the analog is expressed as a fraction of the ability of the corresponding ceramide, either C_{16}-Cer or C_8-Cer. The line drawn is not fit to the

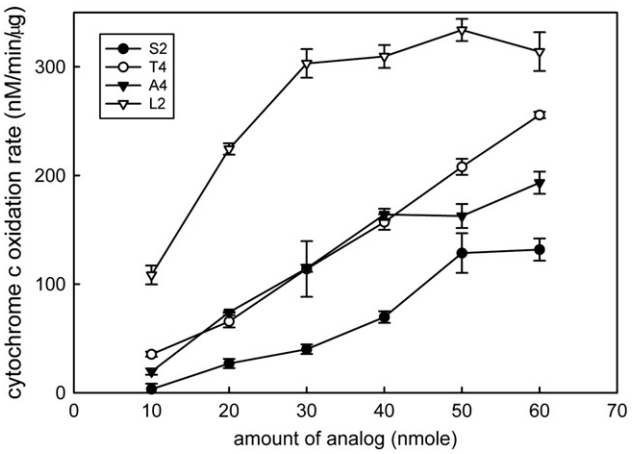

Fig. 3. Examples of dose–response curves of the analogs used. The cytochrome *c* oxidation rate was used to assess the permeability of the MOM to proteins. The indicated amount of analog was added to 0.7 mL of a mitochondrial suspension (see Section 2.4).

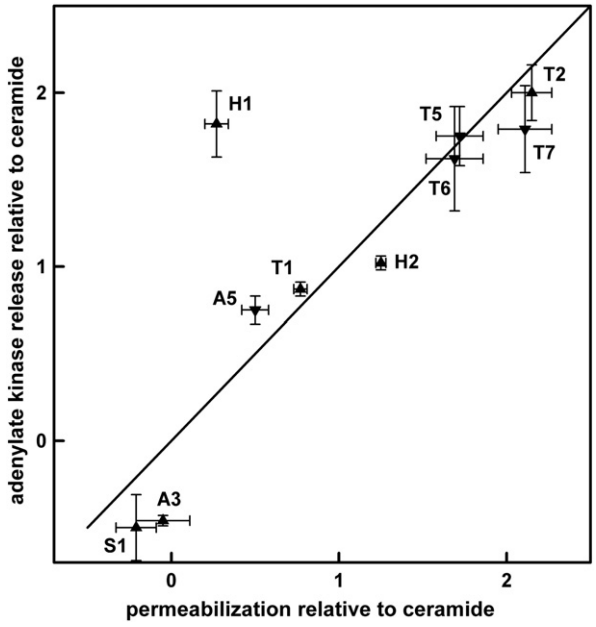

Fig. 4. Correlation between changes in MOM permeability and adenylate kinase release by analogs. The "permeabilization relative to ceramide" is the rate of cytochrome *c* oxidation induced by the analog divided by that induced by ceramide (C_{16}-Cer for triangles and C_8-Cer for inverted triangles) under the same conditions. "adenylate kinase release relative to ceramide" is the activity of adenylate kinase released from mitochondria by analog addition divided by that released by ceramide. The error bars are standard error of at least three experiments.

data but is a theoretical line for a 1:1 correlation between the two experimental results.

The MOM permeabilization is dependent on the extent of insertion of the analog into the mitochondria, the propensity for channel formation, and the stability of the channels. Typically, only 0.3% to 1% of the added analog actually inserted into the mitochondrial membranes (Table 3). Phytoceramide was the exception with nearly 5% insertion. The extent of insertion helped to interpret the observed ability of an analog to permeabilize the MOM.

3.1. Ability of analogs to permeabilize the MOM to proteins

Changes in the non-polar portions of ceramide did not interfere with channel formation. The analogs of ceramide having a shorter *N*-acyl chain **{L1}** or a shorter sphingosine backbone **{L2, L5}** were more potent in permeabilizing the MOM than C_{16}-Cer (Table 2). For C_2-ceramide [4] the additional potency was attributed to an enhanced ability to incorporate into the mitochondrial membrane. That is not the case for C_{10}-ceramide **{L1}** (Table 2, column 5) as the permeabilization was increased 6 fold despite no difference in the degree of incorporation into the MOM. Increasing the effective bulk of the hydrocarbon chain by using fluorescently labeled C_6-NBD-ceramide **{L4}**, or $C_{18:1}$-Cer **{L6}** with a *cis* double bond in the middle of the acyl chain, inhibited cytochrome oxidase activity. After correction for the inhibition, channel formation by $C_{18:1}$-Cer **{L6}** was indistinguishable from that of C_{16}-Cer (Table 2).

Major alterations in ceramide's *trans* double bond were also well tolerated (Tables 2 and 5). Some of these were analogs of C_8-ceramide. Under identical treatments, C_8-Cer **{L3}** permeabilized the MOM to cytochrome c 36% of the maximal permeabilization, whereas the *cis* isomer **{T6}** resulted in a 61% of maximal permeabilization (Table 5). An analog with an extra double bond (6*E*) in conjugation with the first (**{T5}**) permeabilized the outer membrane to the same extent as the *cis* isomer **{T6}**. Moving the 4*E* double bond to a position between the two hydroxyl groups by putting it at the C3 position and moving the C3-hydroxyl group to the C5 position **{T7}** did not prevent MOM permeabilization. Similar results were obtained with analogs of C_{16}-Cer. C_{16}-phytoceramide **{T2}**, where the 4*E*-double bond is replaced by a C4-hydroxyl group, had a 2-fold higher ability to permeabilize the MOM as compared to C_{16}-Cer but this can be more than accounted for by an enhanced ability to insert into the MOM (Table 3). Replacing the 4*E*-double bond by a C4,C5-triple bond **{T3}** also did not significantly affect the ability of the molecule to permeabilize the MOM. Moving the double bond farther down the chain **{T1}** to a position that does not form an allylic system results in an enhanced MOM permeabilization, despite a substantial reduction in its ability to insert into mitochondria. Hence the location, conformation, and degree of unsaturation do not have significant effects on channel-forming ability.

The amide linkage in ceramide is proposed to have similar organizing effects as the amide linkages in proteins [35]. The hydrogen-bonding ability of this linkage was proposed to organize ceramide monomers into columns. We found that increasing the hydrogen-bonding ability of this region by introducing a "urea" linkage **{A4}** resulted in an enhanced ability to permeabilize the MOM (Table 2). Moreover, reducing the hydrogen-bonding capacity by using C_8- and C_{16}-ceramines **{A1, A2},** which differ from ceramide by having an amino instead of an amide group, eliminated the molecule's ability to permeabilize MOM to proteins. Since both of these ceramines strongly inhibit cytochrome oxidase activity, release of adenylate kinase from the mitochondrial intermembrane space was measured. The ceramines caused no significant release of adenylate kinase. For C_{16}-ceramine, kinase release was -0.6 ± 7% for the highest dose tested (8 nmol/μg mitochondrial protein). C_8-ceramine was much more effective at releasing carboxyfluorescein from liposomes than C_8-Cer (Table 4) showing that it readily forms channels but these are very small. Methylation of the amide nitrogen, affording *N*-methyl-C_{16}-Cer **{A3}**, drastically reduced but did not completely eliminate the ability of the molecule to permeabilize the MOM to cytochrome *c* (Table 2). The partitioning of **{A3}** into mitochondria was slightly reduced, however the reduced insertion into the membrane of this analog could not account for the extent of its loss of function.

The ability of **{A3}** to form channels, even at a much reduced potency raises a severe problem with the working model of the ceramide channel where the hydrogen bonding from the amide nitrogen is essential to the overall structure. In the model, the amide nitrogen of one ceramide molecule forms a hydrogen bond with the carbonyl group of another to form ceramide columns. Methylation of the amide nitrogen as in **{A3}** would effectively prevent such interactions. However, in molecular dynamic simulations performed by Andriy Anishkin, whereas the working model of the ceramide channel is the predominant form arising from such simulations, other, minor forms were also detected. In some of these the carbonyl oxygen is not hydrogen bonding with the amide hydrogen of

Table 3
Extent of delivery of ceramide and its analogs to mitochondrial membranes. The indicated amount of lipid was added to a mitochondrial suspension (160 μg protein). The percent of the added lipid that incorporated into mitochondria is shown as mean ± S.E. of 4 trials or the values of individual trials. Column 4 shows the extent of analog insertion when added with equal amounts of C_{16}-Cer. The insertion of C_{16}-Cer was not affected by the presence of the analog. Column 5 is the *t*-test probability value obtained when comparing results in column 3 and 4.

Compound	nmoles added	% incorporation	% incorporation in the presence of C_{16}-Cer	*P* value
D-C_{16}-Cer	56	1.04 ± 0.23		
L-C_{16}-Cer {S1}	56	0.41 ± 0.06		
C_{10}-Cer {L1}	66	0.95 ± 0.07	2.45 ± 0.34	0.01
Phytoceramide {T2}	54	4.78 ± 0.80	1.64 ± 0.36	0.004
N-Me-C_{16}-Cer {A3}	54	0.74, 0.85		
1-O-Me-C_{16}-Cer {H1}	54	1.00, 1.25		
3-O-Me-C_{16}-Cer {H2}	54	0.35, 0.95		
15E-C_{16}-Cer {T1}	56	0.23, 0.42		

Table 4
Comparison of channel-forming activity in mitochondria and liposomes. Liposomes and mitochondria were treated with ceramide analogs to assess the latter's ability to permeabilize membranes. For the liposomes (column 3) the % release of contents was performed at 2 different doses: 87 and 147 nmol per 2.5 mL of liposome suspension. For the MOM permeabilization (column 4) results are expressed as a % permeabilization achieved by hypotonic shock. The dose used was 0.19 nmol/μg protein. Measurements of adenylate kinase release (column 5) are expressed as percent of the kinase activity released following treatment with 0.25 nmol/μg protein.

Compound	Code	Liposome % release	MOM % perm.	Adenylate kinase % release
(2*S*,3*R*,4*E*) C_8-ceramide	L3	17 ± 2 22 ± 3	36 ± 4	24 ± 2
(2*S*,3*R*,4*E*) C_8-ceramine[a]	A2	100	N/D	none
(2*S*,3*R*,4*E*) C2-OCH_3-C_8-ceramide	A5	18 ± 2 24 ± 3	18 ± 3	18 ± 2
(2*S*,3*R*,4*E*,6*E*)C_8-ceramide {diene}	T5	32 ± 3 40 ± 3	62 ± 5	42 ± 4
(2*S*,3*R*,4*Z*) C_8-ceramide {*cis* analog}	T6	37 ± 3 47 ± 4	61 ± 6	39 ± 7
(2*S*,5*R*,3*E*) C_8-ceramide	T7	36 ± 3 46 ± 4	76 ± 6	43 ± 6

[a] Release from liposomes was complete with as little as 15 nmol per 2.5 mL of liposome suspension. MOM permeabilization could not be done (N/D) because of strong inhibition of cytochrome oxidase.

the adjacent ceramide but hydrogen bonding with a C1-hydroxyl through a water bridge (e.g. Fig. 3S). Thus it may be possible for **{A3}** to form a similar structure.

The C1 and C3 hydroxyl groups have been proposed to stabilize channel structure via hydrogen bonds with the corresponding functional groups on adjacent ceramide molecules. Analogs of these functional groups were utilized to determine the contribution of these groups to the channel structure. *O*-Methylation of the C1-hydroxyl group **{H1}** was chosen because the methyl group should prevent this hydroxyl group from donating a hydrogen bond. The methylation of the C1 hydroxyl resulted in an almost complete loss of any stable MOM permeabilization despite no change in ability to insert into mitochondria (Table 4). When the ability of **{H1}** to release adenylate kinase was tested, it was almost double that observed with C_{16}-Cer indicating that twice as many mitochondria were permeabilized, if only transiently, by **{H1}**. When reconstituted into planar membranes, **{H1}** produced conductances that were transient (vide infra) as opposed to the growing conductances observed with C_{16}-Cer (Fig. 8c). These were similar to those published for sphingosine [36] except that these are large enough to allow the release of adenylate kinase (Fig. 4).

Unlike **{H1},** methylation at the C3-hydroxyl **{H2}** produced functional properties very similar to those of C_{16}-Cer (Table 2). Both the cytochrome *c* oxidation assay and the adenylate kinase release assay produced results indistinguishable from those of C_{16}-Cer. The importance of the location of the C3-hydroxyl group and the stereochemistry of the adjacent chiral center were tested by relocating the hydroxyl to the C5 position **{T7}** and by changing configuration from (2*S*,3*R*)-C_{16}-Cer to (2*S*,3*S*)-C_{16}-Cer **{S2}**, respectively. Neither of these alterations had a large effect on the ability of these molecules to permeabilize MOMs of isolated mitochondria (Table 2). Thus the location and orientation of the C3-hydroxyl can be changed with minimal consequences. By sharp contrast, converting the (2*S*,3*R*)-C_{16}-Cer to (2*R*,3*S*)-C_{16}-Cer **{S1}** (i.e. an additional change in the chirality at C2) greatly reduced its ability to permeabilize MOMs, consistent with the importance of the C1-hydroxyl group (Table 2). Unlike the results with **{H1}**, **{S1}** was unable to permeabilize the MOM or release adenylate kinase at 1 nmol/μg protein and produced only 16% of the permeabilization of C_{16}-Cer at 3 nmol/μg protein. The amount of insertion was reduced by a little over half but not enough to account for the large reduction in ability to permeabilize the MOM. Thus, the stereochemistry of ceramide that limits the possible and preferred positions of its polar groups [35], can also influence the propensity for channel formation in the MOM.

3.2. Interactions between D-e-C_{16}-ceramide and its analogs

Isolated mitochondria were treated with either C_{16}-Cer alone or the analog alone, or an equimolar mixture of C_{16}-Cer and the analog at half the dose. Thus, the total amount of sphingolipid added was kept constant. The ability of each of the three treatments to permeabilize the MOM to cytochrome *c* was measured. Examples of the results are shown in Fig. 5. For **{A4}** and **{L2}** the simultaneous presence of both lipids (designated as both) yielded a higher rate of cytochrome *c* oxidation (and therefore a higher permeability) than the average of the individual treatments (avg), thus indicating synergy. The converse was true for **{T4}**, indicating antagonism. For **{S2}** there was no significant difference, indicating neutrality or no cooperativity. Depending on the experimental set, 40 nmol or 60 nmol of lipids were utilized (as indicated in Table 5). The permeability resulting from the combined treatment ("combined effect" in Table 5) was compared to the "expected average" which is the average of the permeabilities observed with the individual sphingolipid treatments. The ratio is reported in Table 5 along with the *P* values of statistical significance and the interpretation of the results. Ratios significantly

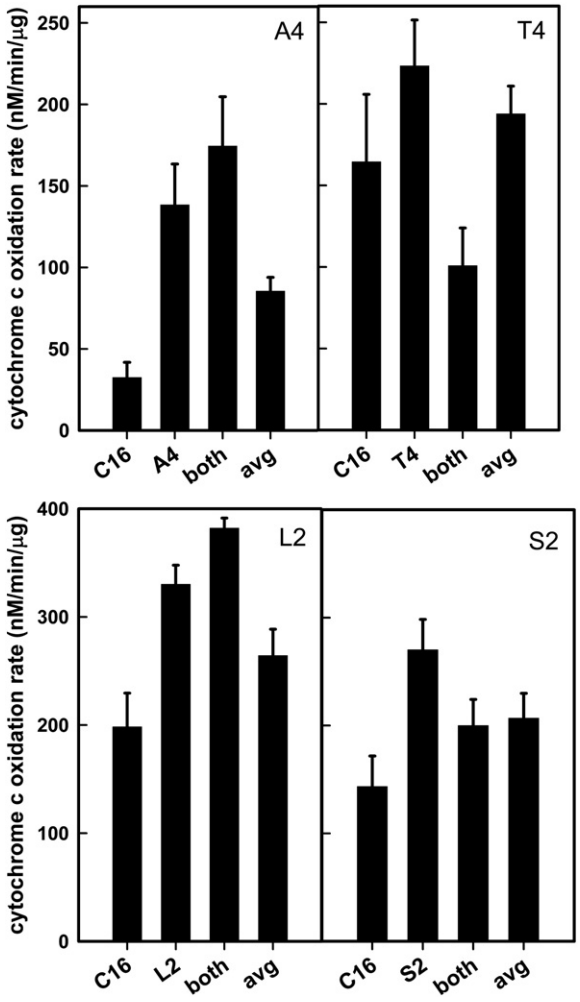

Fig. 5. Cooperativity between analogs and C_{16}-Cer. For an individual addition, a total of 40 nmol was used. For combined additions (both), 20 nmol of each was used. The average bar (avg) shows the average of the results obtained with each lipid alone. The statistics are shown in Table 5. The individual and combined additions for each analog were performed with the same batch of mitochondria under the same conditions to avoid the variability in sensitivity to ceramide found among mitochondrial preparations.

Table 5
Cooperativity between C_{16}-ceramide and its analogs. The analog was mixed in equimolar quantities with C_{16}-Cer and the permeabilization of the MOM was compared to the average permeabilization observed with equal total amounts of either C_{16}-Cer or the analog alone. At least 3 experiments were performed for each condition and *P* values for the *t*-tests are listed. Using 95% confidence, ratios significantly greater than 1 are labeled synergistic; significantly less than 1, antagonistic; not significantly different, neutral.

Compound	Code	Combined effect expected average	*P* value	Nature of interaction
(2*R*,3*S*,4*E*) C_{16}-ceramide	S1	0.33	0.0005	Antagonistic
(2*S*,3*S*,4*E*) C_{16}-ceramide	S2	1[a]	0.36	Neutral
(2*S*,3*R*,4*E*) *N*-methyl-C_{16}-ceramide	A3	0.21	0.003	Antagonistic
(2*S*,3*R*,4*E*) C_{16}-urea-ceramide	A4	1.5[a]	0.015	Synergistic
(2*S*,3*R*,4*E*) 3-O-methyl-C16-ceramide	H2	1.0	0.25	Neutral
(2*S*)-3-keto-C_{16}-dh-ceramide	H3	1.0	0.41	Neutral
(2*S*,3R,15E) C_{16}-dh-ceramide	T1	1.3	0.15	Neutral
(2*S*,3*R*,4*R*) C_{16}-phytoceramide	T2	0.52[a]	0.009	Antagonistic
(2*S*,3*R*) C_{16}-4,5-tb-ceramide	T3	0.95[a]	0.33	Neutral
(2*S*,3*R*,4*E*) C_{16}-(4,5-allene)-ceramide	T4	1.3	0.06	Neutral
(2*S*,3*R*,4*E*) C_{10}-ceramide	L1	1.5[a]	0.04	Synergistic
(2*S*,3*R*,4*E*) 13C/C_{16}-ceramide	L2	1.4[a]	0.02	Synergistic
N-palmitoyl-serinol	L5	1.4	0.002	Synergistic

[a] The increase in MOMP resulting from the addition of a total of 3.6 nmol/μg protein of an equimolar mixture of C_{16}-Cer and the specified analog was compared to 3.6 nmol/μg protein of either C_{16}-Cer or the analog alone. In the other experiments, 5.6 nmol/μg protein were used.

greater than 1 indicate synergy and ratios significantly less show antagonism.

A subtle change, such as the replacement of the 4*E* double bond of ceramide with a C4,C5-triple bond **{T3},** resulted in a neutral effect when combined with C_{16}-Cer (Table 5). Experiments with the diastereomer **{S2}** (2*S*,3*S* as opposed to 2*S*,3*R* for C_{16}-Cer) were also consistent with simple neutrality (Fig. 5 and Table 5).

Treating mitochondria with a mixture of C_{16}-Cer and the shorter chain analog, 13C/$C_{16:0}$ {**L2**} resulted in a permeabilization that was greater than the average of treatments with individual compounds (Fig. 5). Similar results were obtained with other short-chain analogs **{L1, L5}** (Table 5) and with urea-ceramide **{A4}.**

Mitochondria treated with an equimolar mixture of ceramide and phytoceramide **{T2}** achieved a much reduced level of permeabilization than expected from averaging the individual treatments (Fig. 5, Table 5). This inhibition was also found between phytoceramide **{T2}** and L-e-C_{16}-Cer **{S1}** (data not shown). A similar antagonistic interaction was found between C_{16}-Cer and either *N*-methyl-C_{16}–Cer **{A3}** or the enantiomer, (2*R*,3*S*) **{S1}**.

The type and degree of cooperativity correlates with the channel-forming ability of the analog. A plot of the channel-forming potency relative to that of C_{16}-Cer versus the cooperativity ratio from Table 5 shows the strong correlation (Fig. 6). The upper right quadrant contains data from the analogs showing synergy and higher propensity for channel formation whereas the lower right quadrant contains data from those displaying antagonism and lower channel-forming propensity. Analogs showing no cooperativity and essentially similar channel-forming propensity to C_{16}-Cer tend to cluster at the "origin". The other two quadrants are essentially vacant.

The permeabilization of the MOM following the dispersal of ceramide or an analog must involve at least two processes: insertion and self-assembly. The cooperativity could take place at one or both of these. The influence of combined delivery on the insertion of the sphingolipids was assessed for one analog showing synergy **{L1}** and one showing antagonism **{T2}** (Table 3). The presence of C_{16}-Cer influenced the ability of the analogs to insert into the MOM in harmony with the observed cooperativity. The amount of **{T2}** that inserted when combined with C_{16}-Cer was one third of that measured following its individual addition whereas the insertion of **{L1}** doubled. The insertion of C_{16}-Cer was not significantly affected by the presence of the analog.

The antagonism observed in mitochondrial experiments was also evident in experiments with liposomes, showing a direct interaction between these lipids. Premixing C_{16}-Cer and C_{16}-phytoceramide **{T2}** resulted in a much smaller permeabilization of liposome membranes than phytoceramide **{T2}** alone (Fig. 7).

3.3. Channel formation in phospholipid membranes

To directly observe channel formation by ceramide analogs and to gain insight into their stability and dynamics, experiments were performed in defined systems consisting of phospholipid membranes: planar membranes and liposomes. In planar membranes, channel formation was monitored as changes in conductance to K^+ and Cl^- ions. In liposomes, the release of carboxyfluorescein and the quenching agent, DPX, was used to assess the permeabilization of single-walled liposomes by the analogs. In both of these experimental systems, the analogs that were able to permeabilize the MOM were also able to permeabilize phospholipid membranes that were free of proteins, demonstrating that the analogs form channels rather than inducing MOM proteins to form channels.

Most of the analogs that could permeabilize the MOM produced conductances in planar membranes with similar characteristics to those of C_{16}-Cer. Examples for phytoceramide **{T2}** and urea-ceramide **{A4}** are shown in Fig. 5. Channel formation occurred after a lag phase and usually required a few separate additions. Fig. 8A shows how a sustained conductance developed after a final addition

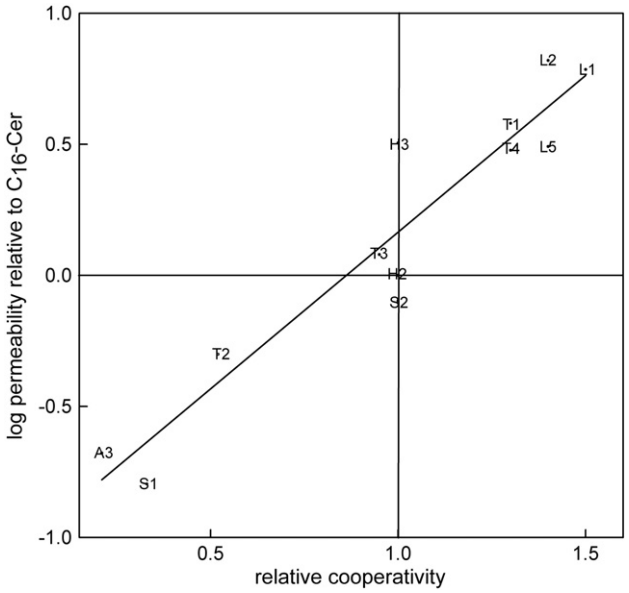

Fig. 6. Correlation between degree of cooperativity and ability of an analog to permeabilize the MOM. Relative cooperativity is from column 3 of Table 5. The permeability relative to C_{16}-Cer is from Table 2 column 3 after dividing by 100 and taking the log.

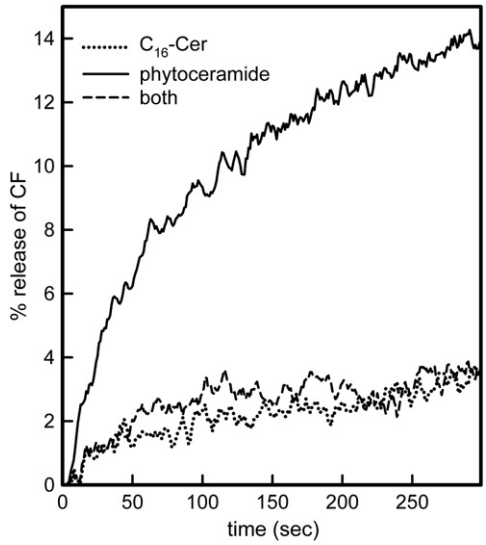

Fig. 7. Permeabilization of liposomes by C_{16}-Cer, C_{16}-phytoceramide {T2}, or the two together.

of 1 nmol of **{A4}**. The conductance increased in steps of varying size until it reached a plateau. Sometimes the increase was rapid, reaching a high conductance (Fig. 8B). At the reduced gain required to observe the total conductance the increase appears to be very smooth. Addition of La^{+3} resulted in channel disassembly after a variable delay (Fig. 8B), which is similar to the effect of La^{+3} on a C_{16}-ceramide channels as previously reported [10]. The variable delay is characteristic of a stochastic process [10] and is also consistent with the formation of a single channel that enlarges in size. Most of the analogs appear to form a single large channel in the planar membrane (data not shown), as was demonstrated for ceramide [10].

Marked exceptions were the behaviors of the conductances produced by 1-O-methyl-C_{16}-ceramide **{H1}**, *N*-methyl-C_{16}-ceramide **{A3}** and $C_{18:1}$-Cer **{L6}**. With these compounds, the conductance rose rapidly but was transient, declining and returning to the baseline shortly thereafter. This behavior was often observed multiple times in the same membrane. Only occasionally would a prolonged conductance form. The analog with the shortest conductance bursts was **{H1}** (Fig. 8C). The figure shows samples of conductance burst recorded within a 40 min period of activity. **{L6}** was at the other end of the spectrum, producing greater conductances but these also tended to decay (Fig. 8D). The addition of more sample produced a second transient conductance. **{A3}** was intermediate between these (data not shown). The behavior of these analogs is consistent with a less stable structure and in agreement with the observations made with isolated mitochondria. **{H1}** produced virtually no permeability; {**A3}** had a much diminished permeabilizing ability (21% of that induced by C_{16}-cer, Table 2); **{L6}** produced an effective permeabilization similar to C_{16}-Cer. Clearly the channel dynamics are not detectable in mitochondrial experiments and only the average permeability to cytochrome c is assessed.

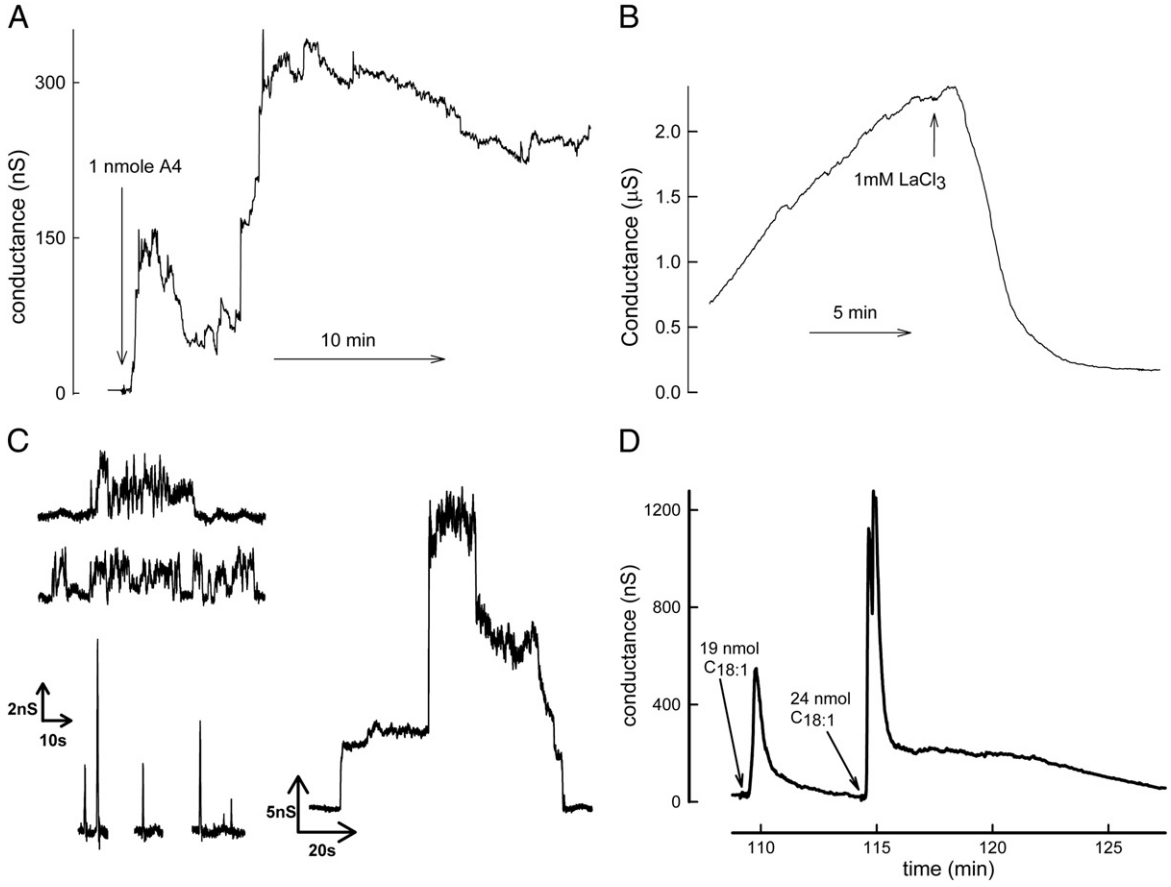

Fig. 8. Electrophysiological recording of conductances formed by ceramide analogs in planar phospholipid membranes. A. The formation of a channel by urea ceramide **{A4}**. Equal amounts of the analog were added at intervals (for a total of 4.6 nanomoles) with the last shown in the figure. B. The formation of a C_{16}-phytoceramide **{T2}** channel and its partial disassembly by the addition of $LaCl_3$. Channel formation followed the addition of 0.46 nmol of C_{16}-phytoceramide **{T2}**. C. Segments of conductance transients observed after addition of 1 nmol of ceramide methylated at the C1-hydroxyl **{H1}**. The bursts shown were observed over a 40 min time period. D. Transient channels formed by **{L6}** $C_{18:1}$-ceramide. A total of 25 nmol of $C_{18:1}$ was added at intervals and similar patterns of channel growth and disassembly were seen after each addition. In all cases the transmembrane voltage was clamped at 10 mV.

In general, liposome permeabilization experiments and adenylate kinase release experiments produced results in agreement with mitochondrial permeability measurements (Table 4 and Fig. 4). **{H1}** and the ceramines **{A1}** and **{A2}** were the exception. **{A2}** induced the maximal release of liposomal contents, but did not facilitate the release of adenylate kinase from the mitochondrial intermembrane space (Table 4). The fact that ceramine can permeabilize liposomes to carboxyfluorescein, but did not permeabilize the MOM to adenylate kinase is consistent with its formation of small channels capable of allowing small molecules to cross membranes, but not large enough to allow the passage of proteins. These conductances resemble those published for sphingosine [38]. Like **{H1}**, these conductances did not grow in size but returned to the baseline and were likely the result of the formation of small pathways such as the toroidal structures induced by amphipathic structures [12–14]. Unlike **{H1}** the transient conductances did not become large enough to release adenylate kinase from mitochondria.

4. Discussion

The data presented show that the structure of ceramide can be altered in a number of ways without losing the ability of the molecule to permeabilize membranes in a manner that is consistent with self-assembly into large channels capable of translocating proteins through membranes. The mitochondrial and planar membrane experiments suggest that many of the analogs form large, stable channels. The results indicate the relative importance of specific structural features of ceramide for channel formation, namely the differential importance of the hydroxyl groups, the role of the *trans* double bond, and the importance of the stereochemistry.

4.1. Effect of chain length on ceramide channel formation

Physiologically, the length of the *N*-acyl chain of ceramide is clearly very important [37,38]. For example, the ceramide synthases show strong specificity for different acyl-CoA substrates [39–42]. Some preferentially produce long-chain ceramides such as C_{16}-Cer, while others preferentially produce very long-chain ceramides such as C_{24}-Cer [40,41]. Many enzymes that metabolize ceramide do not recognize C_2-Cer [43,44]. Yet, with regard to the ability to form channels, the length of the *N*-acyl chain was found to be relatively unimportant [1,3]. After compensating for the difference in delivery to the mitochondrial membranes, the potency of C_{16}-Cer and C_2-Cer were found to be indistinguishable [4]. Here we tested analogs having shorter *N*-acyl chains {**L1, L3}** and shorter sphingoid base backbones **{L2, L5}**. The results indicate that these can also form permeability pathways in membranes in a manner consistent with channels and interact synergistically with ceramide. For **{L1}**, the synergy arises from the ability of C_{16}-Cer to aid in the insertion of **{L1}** into mitochondria.

It is important to note that the minimal ceramide analog, N-palmitoyl-serinol **{L5}**, functions very well with only one aliphatic chain. Thus, one might ask why natural ceramides have such a large amount of apolar mass. The simplest answer would be that the extra bulk anchors the lipid in the membrane, limiting spontaneous, uncatalyzed motion between membranes of different organelles.

4.2. Effect of modifications relating to the trans double bond and hydroxyl groups

An important feature in the ceramide structure is the C4,C5-*trans* double bond in the sphingoid base backbone [35,45]. For permeabilization of the MOM, many changes were well tolerated, namely conversion of *trans* to *cis*, displacement of the double bond relative to the adjacent hydroxyl, and replacement of the double bond by a third hydroxyl. Thus, a variety of structures are capable of permeabilizing membranes in a manner consistent with the channels formed by C_{16}-ceramide.

The ability to form stable channels was lost by *O*-methylation of the C1-hydroxyl group **{H1}**. It forms transient pores capable of allowing adenylate kinase release but too short-lived to significantly increase the overall MOM permeability to proteins. The transient conductances were evident in planar membrane experiments. By contrast, *O*-methylation of the C3-hydroxyl group **{H2}** was well tolerated. Similar results with the C3-keto **{H3}** analog provide additional evidence that C3-hydroxyl modifications are well tolerated. Further evidence for a difference in the importance of these two hydroxyl groups comes from results obtained with stereochemical isomers. The diastereomer studied in which "3R" was changed to "3S" **{S2}** showed no change in MOM permeabilizing properties despite a change in orientation of the C3-hydroxyl. However, the enantiomer, with the same change at the C3 position and an additional change from "S" to "R" at the C2 position **{S1}**, was much weaker in its capacity to permeabilize mitochondria. Thus the presence and orientation of the free hydroxyl at C1 is critical to the stability of the channels, indicating that this hydroxyl forms part of a highly organized structure.

4.3. Effect of changes at the amide linkage

The importance of the amide linkage as an organizing unit is supported by the finding that the conversion of an amide chain to an amine-linked chain in ceramine **{A1, A2}** prevents the permeabilization of the MOM to proteins. If the ceramides are arranged in the channel as proposed by the structural model [10,18], then the conversion of the amide linkage to an amine would indeed destabilize the structure by eliminating the hydrogen bonding that has been proposed to be the basis for the columns that make up the channel. By contrast, the greater hydrogen-bonding and ordering ability of a urea linkage according to the structural model would be expected to stabilize the channel, and indeed this analog **{A4}** forms channels (Fig. 8A). The introduction of a methoxy group in the amide region **{A5}** still allowed channel formation, indicating that the modification is tolerated.

N-methyl C_{16}-Cer **{A3}** can still form channels, which is in apparent contradiction to the structural model because the methyl group that replaces the C3 hydroxyl cannot participate in hydrogen bonding. While its ability to permeabilize the MOM is much reduced as compared to C_{16}-Cer and in planar membranes it forms unstable channels, the ability to form channels at all seems to invalidate the structural model of the ceramide channel. However, channel formation by **{A3}** is antagonistic with that of C_{16}-Cer, indicating that structural incompatibilities were introduced by *N*-methylation. Molecular modeling studies show that a channel can be formed with the carbonyl group hydrogen-bonding with the C1-hydroxyl group through a water bridge as shown by the example structure in Fig. 3S. This structure is quite different from the working model of the ceramide channel [18].

4.4. Cooperativity between ceramide and analogs

Combined addition of C_{16}-Cer and an analog showed cooperativity in membrane permeabilization in certain cases: either synergy or antagonism. The cooperativity correlates well with the ability of individual lipids to permeabilize the MOM. Surprisingly, the cooperativity seems to involve the insertion into the MOM. Insertion may be catalyzed by structures formed by sphingolipids in the membrane. Perhaps ceramide forms phases or domains in the membrane that could engage or exclude other analogs depending on the compatibility or incompatibility of the molecular structures (i.e. their ability to bind to each other). Organized structures composed of many sphingolipids would require that each component fit well sterically and in bonding interactions. Thus very similar structures would be

interchangeable, complementary structures would show synergy and poorly compatible structures would show antagonism. Without structural information it will be difficult to understand the molecular basis for the cooperativity.

5. Conclusions

The results of previously published work on ceramide channels strongly suggests that these channels have a highly organized structure, one in which an altered configuration of the polar lipid head region would disrupt the structure. The results presented here identify key functional groups important for ceramide channel formation and structural aspects where changes are tolerated. The C1-hydroxyl is indispensable for channel stability whereas C3-hydroxyl is not critical for channel formation. It is interesting that further elaborations of ceramide in cells involve additions to the C1-hydroxyl rather than the C3-hydroxyl, thus interfering with the propensity to form channels. The amide linkage is also highly important for channel stability. Reducing the length of the hydrocarbon chains favors channel formation and indeed a single chain is sufficient. The allylic system is not necessary and the *trans* double bond does not seem important to the ability to form channels. The sensitivity of channel stability to the stereochemistry at C2 further supports the notion of ceramide channels being highly-organized structures.

Supplementary materials related to this article can be found online at doi:10.1016/j.bbamem.2012.02.010.

Acknowledgments

We gratefully acknowledge the contribution made by Dr. Andriy Anishkin in providing the unpublished supplemental figure (3S). The authors declare no conflict of interests.

This work was supported by grants from the National Science Foundation [MCB-1023008] to MC and from the National Institutes of Health [HL-083187] to RB. L.J.S is supported by a Career Development Award-2 from the Veterans Administration and pilot project funding from a Veteran's Administration REAP. Synthetic lipids and LC-MS/MS analysis of sphingolipids were provided by the Lipidomics Shared Resource, MUSC, supported by NCI Grants: [IPO1CA097132] and [P30 CA 138313] and NIH/NCRR SC COBRE Grant [P20 RR017677]. Laboratory space for Lipidomics Shared Resource in the CRI building of MUSC was supported by NIH Grant [C06 RR018823] from the Extramural Research Facilities Program of the National Center for Research Resources.

References

[1] L.J. Siskind, M. Colombini, The lipids C_2- and C_{16}-ceramide form large stable channels: implications for apoptosis, J. Biol. Chem. 275 (2000) 38640–38644.
[2] J. Stiban, D. Fistere Jr., M. Colombini, Dihydroceramide hinders ceramide channel formation: implications on apoptosis, Apoptosis 11 (2006) 773–780.
[3] L.J. Siskind, R.N. Kolesnick, M. Colombini, Ceramide channels increase the permeability of the mitochondrial outer membrane to small proteins, J. Biol. Chem. 277 (2002) 26796–26803.
[4] L.J. Siskind, R.N. Kolesnick, M. Colombini, Ceramide forms channels in mitochondrial outer membranes at physiologically relevant concentrations, Mitochondrion 6 (2006) 118–125.
[5] H. Birbes, C. Luberto, Y.T. Hsu, S. El Bawab, Y.A. Hannun, L.M. Obeid, A mitochondrial pool of sphingomyelin is involved in TNFalpha-induced Bax translocation to mitochondria, Biochem. J. 386 (2005) 445–451.
[6] C. Garcia-Ruiz, A. Colell, M. Mari, A. Morales, J.C. Fernandez-Checa, Direct effect of ceramide on the mitochondrial electron transport chain leads to generation of reactive oxygen species. Role of mitochondrial glutathione, J. Biol. Chem. 272 (1997) 11369–11377.
[7] C. Rodriguez-Lafrasse, G. Alphonse, M.T. Aloy, D. Ardail, J.P. Gerard, P. Louisot, R. Rousson, Increasing endogenous ceramide using inhibitors of sphingolipid metabolism maximizes ionizing radiation-induced mitochondrial injury and apoptotic cell killing, Int. J. Cancer 101 (2002) 589–598.
[8] L.J. Siskind, L. Feinstein, T. Yu, J.S. Davis, D. Jones, J. Choi, J.E. Zuckerman, W. Tan, R.B. Hill, J.M. Hardwick, M. Colombini, Anti-apoptotic Bcl-2 family proteins disassemble ceramide channels, J. Biol. Chem. 283 (2008) 6622–6630.
[9] V. Ganesan, M.N. Perera, D. Colombini, D. Datskovskiy, K. Chadha, M. Colombini, Ceramide and activated Bax act synergistically to permeabilize the mitochondrial outer membrane, Apoptosis 15 (2010) 553–562.
[10] L.J. Siskind, A. Davoody, N. Lewin, S. Marshal, M. Colombini, Enlargement and contracture of C_2-ceramide channels, Biophys. J. 85 (2003) 1560–1575.
[11] S. Samanta, J. Stiban, T.K. Maugel, M. Colombini, Visualization of ceramide channels by transmission electron microscopy, Biochim. Biophys. Acta 1808 (2011) 1196–1201.
[12] B. Bechninger, Structure and functions of channel-forming peptides: magainins, cecropins, melittin and alamethicin, J. Membr. Biol. 156 (1997) 197–211.
[13] M.S.P. Sansom, Peptides and lipid bilayers: dynamic interactions, Curr. Opin. Colloid Interface Sci. 3 (1998) 518–524.
[14] S. Qian, W. Wang, L. Yang, H.W. Huang, Structure of transmembrane pore induced by Bax derived peptide: evidence for lipidic pores, Proc. Natl. Acad. Sci. U. S. A. 105 (2008) 17375–17383.
[15] G. Basanez, J.C. Sharpe, J. Galanes, T.B. Brandt, J.M. Hardwick, J. Zimmerberg, Bax type pro-apoptotic proteins porate lipid bilayers through a mechanism sensitive to intrinsic monolayer curvature, J. Biol. Chem. 277 (2002) 49360–49366.
[16] B. Schafer, J. Quispe, V. Choudhary, J.E. Chipuk, T.G. Ajero, H. Du, R. Schneiter, T. Kuwana, Mitochondrial outer membrane proteins assist Bid in Bax-mediated lipidic pore formation, Mol. Biol. Cell 20 (2009) 2276–2285.
[17] A. Blicher, K. Wodzinska, M. Fidorra, M. Winterhalter, T. Heimburg, The temperature dependence of lipid membrane permeability, its quantized nature, and the influence of anesthetics, Biophys. J. 96 (2009) 4581–4591.
[18] A. Anishkin, S. Sukharev, M. Colombini, Searching for the molecular arrangement of the ceramide channels, Biophys. J. 90 (2006) 2414–2426.
[19] J. Usta, S. El-Bawab, Z.M. Szulc, Y.A. Hannun, A. Bielawska, Structural requirements of ceramide and sphingosine based inhibitors of mitochondrial ceramidase, Biochemistry 40 (2001) 9657–9668.
[20] C.E. Chalfant, Z.M. Szulc, P. Roddy, A. Bielawska, Y.A. Hannun, The structural requirements for ceramide activation of serine-threonine protein phosphatases, J. Lipid Res. 45 (2003) 496–506.
[21] N. Karasavvas, R.K. Erukulla, R. Bittman, R. Lockshin, Z. Zakeri, Stereospecific induction of apoptosis in U937 cells by N-octanoylsphingosine stereoisomers and N-octylsphingosine. The ceramide amide group is not required for apoptosis, Eur. J. Biochem. 236 (1996) 729–737.
[22] J. Chun, G. Li, H.-S. Byun, R. Bittman, Synthesis of new trans double bond sphingolipid analogues: Δ4,6 and Δ6 ceramides, J. Org. Chem. 67 (2002) 2600–2605.
[23] L. He, H.-S. Byun, R. Bittman, Stereoselective preparation of ceramide and its skeleton backbone modified analogues via cyclic thionocarbonate intermediates derived by catalytic asymmetric dihydroxylation of alpha, beta-unsaturated ester precursors, J. Org. Chem. 65 (2000) 7627–7633.
[24] H.L. Brockman, M.M. Momsen, R.E. Brown, L. He, J. Chun, H.-S. Byun, R. Bittman, The 4,5-double bond of ceramide regulates its dipole potential, elastic properties, and packing behavior, Biophys. J. 87 (2004) 1722–1731.
[25] L. He, H.-S. Byun, R. Bittman, A stereocontrolled, efficient synthetic route to bioactive sphingolipids: synthesis of phytosphingosine and phytoceramides from unsaturated ester precursors via cyclic sulfate intermediates, J. Org. Chem. 65 (2000) 7618–7626.
[26] J. Chun, H.-S. Byun, G. Arthur, R. Bittman, Synthesis and growth inhibitory activity of chiral 5-hydroxy 2-N-acyl-(3E)-sphingenines. Ceramides with unusual sphingoid backbones, J. Org. Chem. 68 (2003) 355–359.
[27] D.F. Parsons, G.R. Williams, B. Chance, Characteristics of isolated and purified preparations of the outer and inner membranes of mitochondria, Ann. N. Y. Acad. Sci. 137 (1966) 643–666.
[28] R. Douce, J. Bourguignon, R. Brouquisse, M. Neuburger, Isolation of plant mitochondria: general principles and criteria of integrity, Methods Enzymol. 148 (1987) 403–415.
[29] L. Wojtczak, A.B. Wojtczak, A. Wronisze, H. Zaluska, Assay for intactness of outer membrane in isolated mitochondria, Acta Biochim. Pol. 19 (1972) 227–234.
[30] M.R. Wieckowski, M. Vyssokikh, D. Dymkowska, B. Antonsson, D. Brdiczka, L. Wojtczak, Oligomeric C-terminal truncated Bax preferentially releases cytochrome c but not adenylate kinase from mitochondria, outer membrane vesicles and proteoliposomes, FEBS Lett. 3 (2001) 453–459.
[31] J. Bielawski, Z.M. Szulc, Y.A. Hannun, A. Bielawska, Simultaneous quantitative analysis of bioactive sphingolipids by high performance liquid chromatography-tandem mass spectrometry, Methods 39 (2006) 82–91.
[32] J. Bielawski, J.S. Pierce, J. Snider, B. Rembiesa, Z.M. Szulc, A. Bielawska, Comprehensive quantitative analysis of bioactive sphingolipids by high-performance liquid chromatography-tandem mass spectrometry, Hum. Meth. 579 (2009) 443–467.
[33] M. Montal, P. Mueller, Formation of bimolecular membranes from lipid monolayers and study of their electrical properties, Proc. Natl. Acad. Sci. U. S. A. 69 (1972) 3561–3566.
[34] M. Colombini, Characterization of channels isolated from plant mitochondria, Meth. Enzymol. 148 (1987) 465–575.
[35] R. Bittman, Synthetic lipids as bioactive molecules: roles in regulation of cell function, in: T.P. Begley (Ed.), Wiley Encyclopedia of Chemical Biology, 4, Wiley & Sons Inc., New Jersey, 2009, pp. 480–504.
[36] M.J. Elrick, S. Fluss, M. Colombini, Sphingosine, a product of ceramide hydrolysis by ceramidase, disassembles ceramide channels, Biophys. J. 91 (2006) 1749–1756.
[37] S.T. Pruett, A. Bushnev, K. Hagedorn, M. Adiga, C.A. Haynes, M.C. Sullards, D.C. Liotta, A.H. Merrill Jr., Biodiversity of sphingoid bases ("sphingosines") and related amino alcohols, J. Lipid Res. 49 (2008) 1621–1639.
[38] P. Megha, T. Sawatzki, R. Kolter, E. Bittman, London, effect of ceramide N-acyl chain and polar headgroup structure on the properties of ordered lipid domains (lipid rafts), Biochim. Biophys. Acta 1768 (2007) 2205–2212.

[39] V. Menuz, K.S. Howell, S. Gentina, S. Epstein, I. Riezman, S. Fornallaz-Mulhauser, M.O. Hengarner, M. Gomez, H. Riezman, J.C. Martinou, Protection of *C. elegans* from hypoxia by HYL-2 ceramide synthase, Science 324 (2009) 381–384.
[40] K. Venkataraman, C. Reibeling, J. Bodennec, H. Riezman, J.C. Allegood, M.C. Sullards, A.H. Merrill Jr., A.H. Futerman, Upstream of growth and differentiation factor 1 (uog1), a mammalian homolog of the yeast longevity assurance gene 1 (LAG1), regulates N-stearoyl-sphinganine (C18-(dihydro)ceramide) synthesis in a fumonisin B1-independent manner in mammalian cells, J. Biol. Chem. 277 (2002) 35642–35649.
[41] Y. Mizutani, A. Kihara, Y. Igarashi, Mammalian Lass6 and its related family members regulate synthesis of specific ceramides, Biochem. J. 390 (2005) 263–271.
[42] E.L. Laviad, L. Albee, I. Pankova-Kholmyansky, S. Epstein, H. Park, A.H. Merrill Jr., A.H. Futerman, Characterization of ceramide synthase 2: tissue distribution, substrate specificity, and inhibition by sphingosine-1-phosphate, J. Biol. Chem. 283 (2008) 5677–5684.
[43] S. El Bawab, J. Usta, P. Roddy, Z.M. Szulc, A. Bielawska, Y.A. Hannun, Substrate specificity of rat brain ceramidase, J. Lipid Res. 43 (2002) 141–148.
[44] D. Wijesinghe, A. Masiello, P. Subramanian, Z.M. Szulc, A. Bielawska, C.E. Chalfant, Substrate specificity of human ceramide kinase, J. Lipid Res. 46 (2005) 2706–2716.
[45] S.C. Philips, G. Triola, G. Fabrias, F.M. Goni, D.B. Dupre, M.C. Yappert, *Cis* vs *trans* ceramides: effects of the double bond on conformation and H bond interactions, J. Phys. Chem. B 113 (2009) 15249–15255.